

Cooperative Payload Estimation by a Team of Mocobots

Haoxuan Zhang^{1,2}, C. Lin Liu^{1,2}, Matthew L. Elwin^{1,2}, Randy A. Freeman^{2,3,4}, and Kevin M. Lynch^{1,2,4}

Abstract—Consider the following scenario: a human guides multiple mobile manipulators to grasp a common payload. For subsequent high-performance autonomous manipulation of the payload by the mobile manipulator team, or for collaborative manipulation with the human, the robots should be able to discover where the other robots are attached to the payload, as well as the payload’s mass and inertial properties. In this paper, we describe a method for the robots to autonomously discover this information. The robots cooperatively manipulate the payload, and the twist, twist derivative, and wrench data at their grasp frames are used to estimate the transformation matrices between the grasp frames, the location of the payload’s center of mass, and the payload’s inertia matrix. The method is validated experimentally with a team of three mobile robots, or mocobots.

Index Terms—inertial property, payload estimation, mocobot, robot cooperation, human-robot collaboration

I. INTRODUCTION

CONSIDER a scenario in manufacturing, logistics, or construction where a large, substantially rigid payload must be manipulated in all six degrees of freedom (dof), perhaps for an assembly or loading task. Multiple distributed contacts with the payload are required, to respect the workspace and wrench limits of any single manipulator and to minimize stress concentrations for heavy or fragile payloads. If the manipulation task is not one that is easily automated (e.g., it is not a repetitive task performed in a structured environment), then one or more human operators can physically collaborate with a team of mobile cobots, or mocobots [1]. The partnership combines the mocobots’ physical strength with human perception and adaptability (Figure 1).

First, a human guides the mobile manipulators to grasp locations on the common payload. Once the grasps are established, to provide optimal model-based assistance to the human, or for high-performance autonomous manipulation, the robots should be able to discover where the other robots are attached to the payload, as well as the payload’s mass and inertial properties.

In previous work [1], much of this information was provided to the mocobots in advance of manipulation. In this paper, we describe a method for the robots to discover this information. The robots cooperatively manipulate the payload, and the twist, twist derivative, and wrench data at their grasp frames



Fig. 1: Three Omnid mocobots collaborate safely and intuitively with a human operator on a simulated plane wing assembly task.

are used to estimate the transformation matrices between the grasp frames, the location of the payload’s center of mass, and the payload’s inertia matrix. The method is validated experimentally with a team of three mocobots.

A. Related Work

A “mocobot” is a mobile variant of the “cobot,” robots designed for physical collaboration with humans, originally introduced in [2]. Mocobots enhance cobots with mobility for diverse tasks. The Omnid mocobot, designed for human-multirobot collaborative manipulation, is described in [1].

The work in this paper extends previous work by providing a method for discovering payload kinematic and inertial properties, building on previous work in cooperative robot manipulation and payload estimation.

1) *Cooperative Robot Manipulation*: Cooperative robot manipulation involves multiple robots working together to manipulate objects, with applications in manufacturing, construction, and hazardous environments [3–6]. Various control architectures ranging from centralized to distributed systems, including those with no explicit communication, have been utilized for manipulation tasks [7–10].

Approaches like haptic feedback for leader-follower formations [11] and force amplification strategies [12] have been explored. Recent advancements include machine learning techniques to enhance human-robot interaction and adaptability [13, 14]. Some systems use distributed adaptive control of omnidirectional mobile bases equipped with robot arms to autonomously transport payloads [15, 16]. Other configurations include customized robots for collaborative rigid-body

All authors are affiliated with Northwestern University, Evanston, IL 60208 USA. (emails: haoxuanzhang2024@u.northwestern.edu, lin.liu@u.northwestern.edu, elwin@northwestern.edu, freeman@northwestern.edu, kmlynch@northwestern.edu)

¹Department of Mechanical Engineering, ²Center for Robotics and Biosystems, ³Department of Electrical & Computer Engineering, ⁴Northwestern Institute on Complex Systems

manipulation [17] and strategies for manipulating deformable payloads [18].

2) *Payload Estimation*: Knowledge of payload properties, particularly the center of mass (CoM) and inertia matrix, is crucial for the dynamic performance and stability of robotic systems. Early research on payload inertia matrix estimation involved suspending payloads and measuring oscillation periods, which provided reliable results for vehicles and aircraft [19–23]. However, these techniques are impractical for robotic applications, especially in dynamic and unstructured environments.

In the field of robotics, force-torque sensors, combined with Newton-Euler equations, have become a standard tool for the estimation of inertial properties by a single robot [24]. For the case of manipulation by multiple mobile manipulators, decentralized approaches have been developed for estimating properties of the common payload [25, 26]. In [25], the robots cooperatively estimate the centroid of the payload, but the motion is limited to the plane and mass and inertial parameters are not considered. The estimation goals of [26] are closely related to those of this paper, except the algorithms described in that work do not consider the orientations of the robots’ grasp frames and have only been tested in simulation.

B. Contributions

This paper presents a methodology for using a group of mobile robots to discover properties of a rigid-body payload, including the robots’ unknown relative grasp frames on the payload and the payload’s mass, center of mass, and inertia matrix. The approach relies on post-processing experimental data collected without the need for expensive and potentially fragile force-torque sensors. The method is validated experimentally on a team of three custom mocobots.

II. COOPERATIVE RIGID PAYLOAD ESTIMATION PROBLEM FORMULATION

A team of N robots grasps the rigid body, defining the coordinate frames $\{1\} \dots \{N\}$ at the grasp locations. Let $T_{i_0i} \in SE(3)$ define the transformation matrix describing frame $\{i\}$, the current location of robot i ’s grasp, relative to a frame $\{i_0\}$, defined as robot i ’s “home” configuration. The configuration T_{i_0i} can be measured by encoders or other sensors on the robot, but the robot has no exteroceptive sensors to directly sense its location relative to other robots or a common world frame.

To determine the properties of the payload and their relative grasp locations, the robots cooperatively manipulate the payload. For example, each robot may attempt to drive its gripper along a periodic reference trajectory using a soft impedance controller. The combination of the reference trajectories should cause the rigid payload to move in all six degrees of freedom, while the impedance control adapts the actual robot trajectories to ensure safe manipulation forces given the unknown connections of the robots to the rigid payload.

Each robot takes measurements at its grasp interface synchronously with the other robots during manipulation. For example, robot i measures the configuration T_{i_0i} , the twist

$\mathcal{V}_i = (\omega_i, v_i) \in \mathbb{R}^6$ measured in $\{i\}$, its time derivative $\dot{\mathcal{V}}_i$, and the wrench $\mathcal{F}_i = (m_i, f_i) \in \mathbb{R}^6$ measured in $\{i\}$. A complete data point for robot i is defined as the tuple $\mathcal{D}_i = \{T_{i_0i}, \mathcal{V}_i, \dot{\mathcal{V}}_i, \mathcal{F}_i\}$. The set of data points collected by robot i at all Q timesteps is denoted $\mathcal{D}_{i*} = \{\mathcal{D}_{iq} \mid q = 1 \dots Q\}$, and the set of data points collected by all robots at timestep q is denoted $\mathcal{D}_{*q} = \{\mathcal{D}_{iq} \mid i = 1 \dots N\}$. The complete data set is denoted $\mathcal{D}_{**} = \{\mathcal{D}_{iq} \mid i = 1 \dots N, q = 1 \dots Q\}$.

The cooperative rigid payload estimation problem can be formulated as follows: given \mathcal{D}_{**} , determine the payload’s mass m ; the configuration of a frame $\{c\}$ at the payload’s center of mass relative to each robot’s grasp frame (T_{1c}, \dots, T_{Nc}) such that the frame $\{c\}$ is aligned with principal axes of inertia of the payload; and the 3×3 positive-definite inertia matrix \mathcal{I} of the payload in the frame $\{c\}$. This information also implies the configuration of each robot’s grasp relative to each other,

$$T_{ij} = \begin{bmatrix} R_{ij} & p_{ij} \\ 0 & 1 \end{bmatrix} \in SE(3), \quad i, j \in \{1, \dots, N\}.$$

Payload estimation requires that the data set \mathcal{D}_{**} be sufficiently rich, e.g., the manipulation must cause payload rotations that make estimation of the grasp kinematics and inertial properties well posed. Grasp twist and acceleration data \mathcal{V}_i and $\dot{\mathcal{V}}_i$ may be obtained by using filtered encoder data, IMUs, accelerometers, or a combination, and the wrench \mathcal{F}_i may be obtained by end-effector force-torque sensors, force/torque sensors at individual robot joints, or other means.

III. ESTIMATION OF PAYLOAD PROPERTIES USING THE OMNID MOCOBOTS

A. Omnid Mocobots and Sequential Estimation

We perform payload estimation using the Omnid mocobots (Figure 2), which are designed for human-robot collaborative manipulation [1]. Each Omnid mocobot consists of a mecanum-wheel mobile base, a 3-dof Delta parallel mechanism driven by series-elastic actuators (SEAs), and a 3-dof passive gimbal wrist. In this paper, the mobile bases are stationary, and all manipulation is performed by the Delta-plus-gimbal manipulators.

The Delta mechanism and gimbal wrist of each Omnid is equipped with encoders, allowing Omnid i to measure its wrist configuration T_{i_0i} . Since the payload is rigidly attached to the gimbal, the wrist configuration and the grasp configuration are equivalent. The twist \mathcal{V}_i and its derivative $\dot{\mathcal{V}}_i$ are calculated by filtering encoder data. Wrenches at the wrist take the form $\mathcal{F}_i = (m_i, f_i) = (0, f_i)$, where the linear force f_i is calculated based on torques measured at the SEA joints and the moment m_i is zero due to the passive gimbal wrist. Data is collected at a fixed sampling rate of 100 Hz.

In principle, all data \mathcal{D}_{**} could be used in a single optimization to simultaneously calculate the configurations of the robot grasps relative to each other, the mass and location of the center of mass of the payload, and the inertia of the payload. In this paper, we adopt a sequenced approach, where we first estimate the grasp kinematics using only twist measurements; then estimate the mass and center of mass using the results of the kinematics estimates and wrench

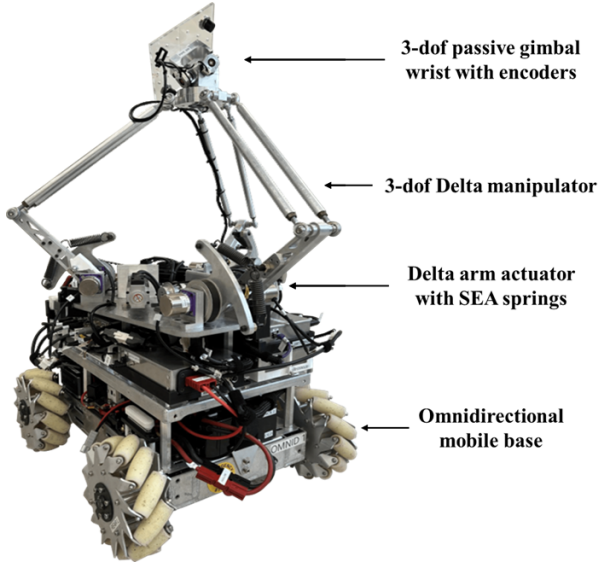


Fig. 2: The structure of the Omnid mocobot.

measurements when the payload is held stationary; and finally estimate the inertial properties using the results of the previous estimates as well as twist, acceleration, and wrench data during manipulation. This approach (a) allows us to use simple least-squares estimation and (b) requires only the data needed for the particular parameters being estimated—for example, wrench and acceleration data is not needed to estimate the robots’ relative grasp frame configurations.

B. Grasp Kinematics

When robots i and j grasp a common rigid body, the twists $\mathcal{V}_i, \mathcal{V}_j$ are related by $\mathcal{V}_i = [\text{Ad}_{T_{ij}}]\mathcal{V}_j$, where $[\text{Ad}_{T_{ij}}] \in \mathbb{R}^{6 \times 6}$ is the adjoint representation of the transformation matrix T_{ij} describing the configuration of the frame $\{j\}$ relative to $\{i\}$ [27]. We write the complete set of twist measurements as $\mathcal{V}_{i*}, \mathcal{V}_{j*} \in \mathbb{R}^{6 \times P}$, i.e., each individual twist measurement \mathcal{V}_i forms a column of the matrix \mathcal{V}_{i*} . Then

$$\mathcal{V}_{i*} = [\text{Ad}_{T_{ij}}]\mathcal{V}_{j*}, \quad (1)$$

or, in expanded form,

$$\begin{bmatrix} \omega_{i*} \\ v_{i*} \end{bmatrix} = \begin{bmatrix} R_{ij} & 0 \\ [p_{ij}]R_{ij} & R_{ij} \end{bmatrix} \begin{bmatrix} \omega_{j*} \\ v_{j*} \end{bmatrix}, \quad (2)$$

where $[p_{ij}] \in \mathfrak{so}(3)$ is the skew-symmetric representation of $p_{ij} \in \mathbb{R}^3$. This equation is the basis for estimating the rotation matrix R_{ij} and the position vector p_{ij} between the two robots.

1) *Rotation Matrix*: Let $\omega_{i*}, \omega_{j*} \in \mathbb{R}^{3 \times P}$ be the angular velocities of the twists measured at each grasp. The relationship between the two sets is

$$\omega_{i*} = R_{ij}\omega_{j*}. \quad (3)$$

The problem is to estimate a rotation matrix \hat{R}_{ij} that best fits the data in Equation (3) by solving the following least-squares problem based on the Frobenius norm:

$$\hat{R}_{ij} = \underset{R_{ij} \in SO(3)}{\text{argmin}} \|R_{ij}\omega_{j*} - \omega_{i*}\|_F^2. \quad (4)$$

This problem is known as Wahba’s problem, which has been solved by the Kabsch-Umeyama algorithm [28–30]. Defining the matrix $X = \omega_{j*}\omega_{i*}^T$, utilizing SVD decomposition to get $X = U\Sigma V^T$, and defining $S = \text{diag}(1, 1, \det(VU^T))$, the solution to the optimization problem is

$$\hat{R}_{ij} = VSU^T. \quad (5)$$

At least three pairs of angular velocities are required to uniquely determine the rotation matrix R_{ij} . We assume the measurement data are sufficiently rich to ensure that X is full rank.

2) *Position Vector*: Let $v_{i*}, v_{j*} \in \mathbb{R}^{3 \times P}$ be the linear velocities of the twists measured at each grasp. By Equation (2), the linear velocities satisfy

$$v_{i*} = [p_{ij}]R_{ij}\omega_{j*} + R_{ij}v_{j*}. \quad (6)$$

Due to the skew-symmetric property $[\omega]p = -[p]\omega$, Equation (6) can be rearranged to

$$v_{i*} = -[R_{ij}\omega_{j*}]p_{ij} + R_{ij}v_{j*}. \quad (7)$$

Plugging in the estimate \hat{R}_{ij} , the estimate \hat{p}_{ij} is found by solving the least-squares problem

$$\hat{p}_{ij} = \underset{p_{ij}}{\text{argmin}} \|[\hat{R}_{ij}\omega_{j*}]p_{ij} - (\hat{R}_{ij}v_{j*} - v_{i*})\|_2, \quad (8)$$

provided $[\hat{R}_{ij}\omega_{j*}]$ is full rank.

The solution $\hat{T}_{ij} = (\hat{R}_{ij}, \hat{p}_{ij})$, via Equations (4) and (8), depends only on pairwise robot data. To obtain a complete and consistent representation of the robots’ relative grasp frames, $N-1$ such solutions are needed, e.g., $\hat{T}_{12}, \hat{T}_{13}, \dots, \hat{T}_{1N}$. Then the configuration of any frame $\{i\}$ relative to another frame $\{j\}$ may be calculated as $\hat{T}_{ij} = \hat{T}_{1i}^{-1}\hat{T}_{1j}$. While this method permits efficient linear least-squares computation, it does not simultaneously take into account all combinations of robots’ twist data nor loop-closure constraints among three or more robots, e.g., $T_{ij}T_{jk}T_{ki} = I$. Such constraints allow squeezing more information out of the collected data at the cost of greater computational complexity and nonlinear optimization.

We employed an iterative gradient-based nonlinear optimization to incorporate all the data and loop constraints to further refine the \hat{T}_{ij} estimates from the original linear least-squares solutions. The optimization minimizes the weighted sum of squared errors from data from all pairwise combinations of grasping frames and all closed loops. Our implementation uses the `scipy.optimize` library and the Broyden-Fletcher-Goldfarb-Shanno method for estimating gradients [31], but other nonlinear optimization methods incorporating combinatorial loop-closure constraints could also be employed [32, 33].

C. Mass and Center of Mass (CoM)

The mass and center of mass are estimated using the grasp kinematics solution and a set of static wrench measurements. A common reference frame $\{s\} \in \{\{1\}, \dots, \{N\}\}$ is selected for the estimation process. We also define a frame $\{s_0\}$ coincident with $\{s\}$ but oriented such that its \hat{z} -axis is opposite the gravity vector $\mathbf{g} \in \mathbb{R}^3$. The center of mass of the payload is located at the origin of a to-be-estimated frame $\{c\}$.

The force and moment static equilibrium conditions are

$$\mathbf{m}\mathbf{g} = -\sum_{i=1}^N R_{s_0i} f_i \quad (9)$$

$$[p_{sc}](R_{ss_0} \mathbf{m}\mathbf{g}) = -\sum_{i=1}^N [p_{si}](R_{si} f_i), \quad (10)$$

where m is the mass of the payload, f_i is the measured force component of \mathcal{F}_i , and p_{sc} and p_{si} represent the origin of $\{c\}$ and $\{i\}$ in $\{s\}$ coordinates, respectively.

To ensure static equilibrium, the payload must be supported by three or more robots, as two Omnidirs cannot resist a moment about an axis through the two grasp frames. Under this condition, the mass m can be estimated using Equation (9) and one or more static measurements by the robots, while p_{sc} can be estimated using Equation (10) and two or more static measurements, provided the orientations of the payload during measurement differ by rotation about an axis not aligned with the gravity vector \mathbf{g} .

Since the robots rigidly grasp the payload, p_{sc} , p_{si} , and R_{si} are constant, and only p_{sc} remains unknown. Given $q = 1 \dots Q$ measurements by the robots, we define the scalars

$$A_q = [0, 0, 1]\mathbf{g}, \quad b_q = -[0, 0, 1] \left(\sum_{i=1}^N R_{s_0i}^q f_i^q \right) \quad (11)$$

and the vectors

$$A = \begin{bmatrix} A_1 \\ A_2 \\ \vdots \\ A_Q \end{bmatrix} \in \mathbb{R}^{Q \times 1}, \quad b = \begin{bmatrix} b_1 \\ b_2 \\ \vdots \\ b_Q \end{bmatrix} \in \mathbb{R}^{Q \times 1}. \quad (12)$$

Plugging this data into the \hat{z} -component of Equation (9), we get

$$A\mathbf{m} = b, \quad (13)$$

which can be solved for the mass estimate \hat{m} using least squares.

Similarly, the data can be plugged into Equation (10) to estimate the center-of-mass location $p_{sc} \in \mathbb{R}^3$:

$$A_q = [R_{ss_0}^q \hat{m}\mathbf{g}] \in \mathbb{R}^{3 \times 3}, \quad b_q = \sum_{i=1}^N [p_{si}](R_{si}^q f_i^q) \in \mathbb{R}^{3 \times 1}, \quad (14)$$

$$A = \begin{bmatrix} A_1 \\ A_2 \\ \vdots \\ A_Q \end{bmatrix} \in \mathbb{R}^{3Q \times 3}, \quad b = \begin{bmatrix} b_1 \\ b_2 \\ \vdots \\ b_Q \end{bmatrix} \in \mathbb{R}^{3Q \times 1}, \quad (15)$$

$$A p_{sc} = b, \quad (16)$$

which can be solved for the estimate $\hat{p}_{sc} \in \mathbb{R}^3$ using least squares.

D. Inertia Matrix

We define a frame $\{b\}$ at the center of mass \hat{p}_{sc} and aligned with $\{s\}$. After estimating the inertia matrix in $\{b\}$, we identify the principal axes of inertia in $\{b\}$, and then define a final center-of-mass frame $\{c\}$ with axes aligned with the principal axes of inertia.

The Newton-Euler dynamics of a rotating rigid body are

$$m_b = \mathcal{I}_b \alpha_b + [\omega_b] \mathcal{I}_b \omega_b, \quad (17)$$

where m_b is the moment acting on the body, $\mathcal{I}_b \in \mathbb{R}^{3 \times 3}$ is the positive-definite inertia matrix of the payload, ω_b is the angular velocity, and α_b is the angular acceleration, all expressed in the frame $\{b\}$. For N robots supporting the payload via linear forces f_i at the gimbals, the moment can be expressed as

$$m_b = \sum_{i=1}^N [p_{bi}](R_{bi} f_i). \quad (18)$$

Equations (17) and (18) can be reorganized to solve for \mathcal{I}_b using linear least squares. Since \mathcal{I}_b is symmetric, it contains six unique elements: \mathcal{I}_{xx} , \mathcal{I}_{xy} , \mathcal{I}_{xz} , \mathcal{I}_{yy} , \mathcal{I}_{yz} , and \mathcal{I}_{zz} . We define

$$\mathcal{I}_{\text{reg}} = [\mathcal{I}_{xx}, \mathcal{I}_{xy}, \mathcal{I}_{xz}, \mathcal{I}_{yy}, \mathcal{I}_{yz}, \mathcal{I}_{zz}]^\top. \quad (19)$$

At timestep q , we construct the matrices $A_q, B_q \in \mathbb{R}^{3 \times 6}$ (based on the angular acceleration $\alpha_b = (\alpha_x, \alpha_y, \alpha_z)$ and angular velocity ω_b measured in $\{s\}$) and the vector y_q based on force measurements at each of the N robots:

$$A_q = \begin{bmatrix} \alpha_x & \alpha_y & \alpha_z & 0 & 0 & 0 \\ 0 & \alpha_x & 0 & \alpha_y & \alpha_z & 0 \\ 0 & 0 & \alpha_x & 0 & \alpha_y & \alpha_z \end{bmatrix}, \quad (20)$$

$$B_q = \begin{bmatrix} 0 & -\omega_x \omega_z & \omega_x \omega_y \\ \omega_x \omega_z & \omega_y \omega_z & \omega_z^2 - \omega_x^2 \\ -\omega_x \omega_y & -\omega_y^2 + \omega_x^2 & -\omega_y \omega_z \end{bmatrix} \quad (21)$$

$$\begin{bmatrix} -\omega_y \omega_z & -\omega_z^2 + \omega_y^2 & \omega_y \omega_z \\ 0 & -\omega_x \omega_y & -\omega_x \omega_z \\ \omega_x \omega_y & \omega_x \omega_z & 0 \end{bmatrix},$$

$$y_q = \sum_{i=1}^N [\hat{p}_{bi}](\hat{R}_{bi} f_{iq}). \quad (22)$$

Combining Equations (17) and (18), the dynamics can be written

$$(A_q + B_q) \mathcal{I}_{\text{reg}} = y_q. \quad (23)$$

For Q measurements, we define

$$X = \begin{bmatrix} A_1 + B_1 \\ A_2 + B_2 \\ \vdots \\ A_Q + B_Q \end{bmatrix} \in \mathbb{R}^{3Q \times 6}, \quad y = \begin{bmatrix} y_1 \\ y_2 \\ \vdots \\ y_Q \end{bmatrix} \in \mathbb{R}^{3Q \times 1}, \quad (24)$$

yielding

$$X \mathcal{I}_{\text{reg}} = y, \quad (25)$$

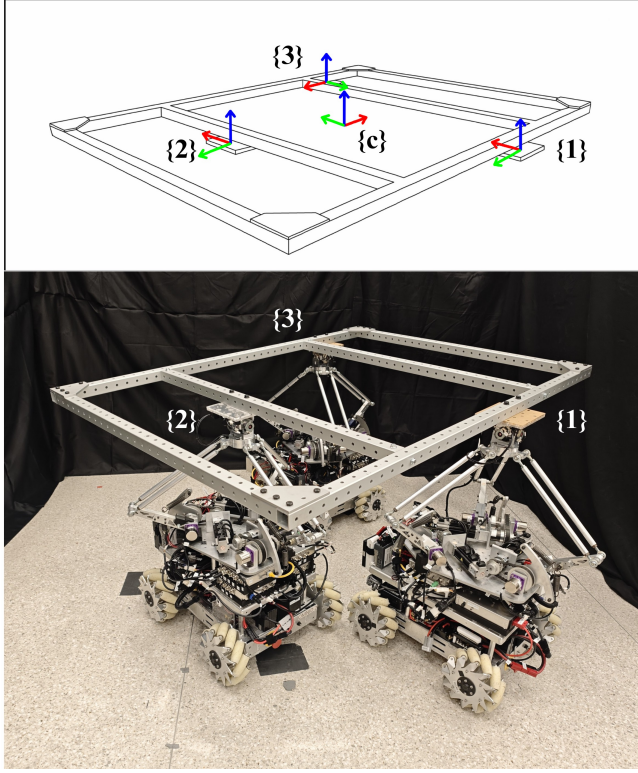


Fig. 3: Frame definition of the robot-payload system for experiments. Frame {1} is chosen as the reference frame {s}. The axes of the frames are visually differentiated by colors with red corresponding to the x -axis, green to the y -axis, and blue to the z -axis.

which $\hat{\mathcal{L}}_{\text{reg}}$ solves in a least-squares sense. The elements of $\hat{\mathcal{L}}_{\text{reg}}$ form the entries of the estimated inertia matrix $\hat{\mathcal{L}}_b$.¹

Let $R_{bc} = [r_1, r_2, r_3]$, where r_i is the i th eigenvector of $\hat{\mathcal{L}}_b$ and {c} is a frame coincident with {b} with axes aligned with the principal axes of inertia. Then the estimated diagonal inertia matrix in {c} is

$$\hat{\mathcal{L}}_c = R_{bc}^T \hat{\mathcal{L}}_b R_{bc}. \quad (26)$$

IV. EXPERIMENTAL IMPLEMENTATION

A. Experimental Configuration

The payload used in the experimental validation is a frame made from ready-tube aluminum extrusion. The payload is attached to the Omnid gimbal wrists, and the attachments remain unchanged during experiments. The overall setup is shown in Figure 3. The Omnid grasp frames are denoted {1}, {2}, and {3}. Frame {1} is selected as the reference frame {s}.

Each 6-dof manipulator consists of a 3-dof Delta mechanism and a 3-dof passive gimbal joint (Figure 4). When the payload is rigidly attached, the top of the gimbal wrist is considered part of the payload. Accordingly, the grasp frame {i} is positioned at the center of the gimbal wrist.

The ground truth values of the transformation matrices, mass, center of mass, and inertia matrix for experimental

¹If noisy data causes the least-squares estimate to produce an $\hat{\mathcal{L}}_b$ with a negative eigenvalue, the inertia estimate can either be discarded or projected to the space of positive semidefinite matrices by performing an eigenvalue decomposition and replacing any negative eigenvalue with a zero eigenvalue.

Rotation Matrix in Axis Angle (deg)	R_{12}	R_{23}	R_{31}
	(0, 0, 0)	(0, 0, 90)	(0, 0, -90)
Position Vector (m)	p_{12}	p_{23}	p_{31}
	(0.647, 0.533, 0)	(0.457, -0.838, 0)	(0.305, 1.105, 0)
Mass (kg), Center of Mass (m), and Principal Axes (deg)	m	p_{1c}	R_{1c}
	11.412	(0.553, 0.172, 0.072)	(0.001, 0.010, -95.016)
Inertia Matrix ($\text{kg}\cdot\text{m}^2$)	\mathcal{I}_{xx}	\mathcal{I}_{yy}	\mathcal{I}_{zz}
	2.258	3.448	5.698

TABLE I: Ground truth values of the experimental configuration.

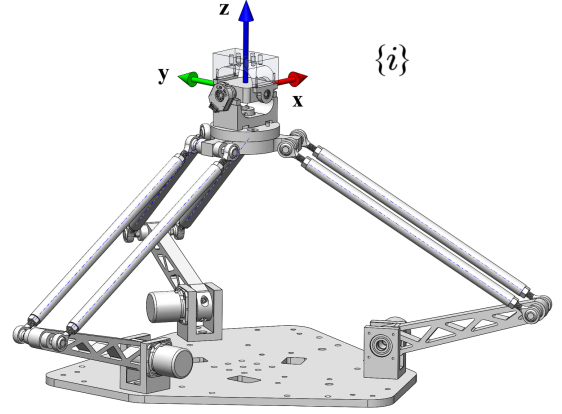


Fig. 4: Frame {i} of the 6-dof manipulator of Omnid i is positioned at the center of the gimbal wrist.

validation were derived from CAD and are summarized in Table I. Rotation matrices are summarized in the axis-angle (exponential coordinates) representation $\omega\beta \in \mathbb{R}^3$, where ω is the unit rotation axis and β is the angle of rotation, expressed in this paper in degrees.

B. Data Processing

Let $\theta = (\theta_1, \theta_2, \theta_3)$ represent the actuated proximal joint angles of the Delta mechanism and $\phi = (\phi_x, \phi_y, \phi_z)$ represent the angles of the gimbal wrist, all measured by encoders. The transformation matrix T_{i_0i} can be derived through forward kinematics as

$$T_{i_0i}(\theta, \phi) = \begin{bmatrix} g(\phi) & h(\theta) \\ 0 & 1 \end{bmatrix}. \quad (27)$$

The twist $\mathcal{V}_i = (\omega_i, v_i)$ is calculated as

$$T_{i_0i}^{-1} \dot{T}_{i_0i} = [\mathcal{V}_i] = \begin{bmatrix} [\omega_i] & v_i \\ 0 & 0 \end{bmatrix} \in se(3). \quad (28)$$

The wrench at {i} is $\mathcal{F}_i = (0, f_i)$, where $f_i = (\partial h / \partial \theta)^{-T} \tau_i$ and τ_i is the Delta's SEA joint torque vector.

The derivative \dot{T}_{i_0i} and the twist derivative $\dot{\mathcal{V}}_i$ are calculated using central differencing post-processing of the 100 Hz estimates of T_{i_0i} and \mathcal{V}_i , respectively. To smooth the data and reduce the effect of amplification of encoder quantization in this numerical differencing, we apply a fourth-order Butterworth low-pass filter to the encoder data prior to calculating the T_{i_0i} estimates. The same filter is applied to smooth the SEA torque data.

Parameters	Absolute Error	
	Mean	Standard Deviation
R_{12} (deg)	1.945	0.292
R_{23} (deg)	2.746	0.552
R_{31} (deg)	1.469	0.690

TABLE II: Experimental results for relative grasp frame rotation matrix estimation. Results are represented in absolute degrees of rotation around the axis that rotates the estimated rotation matrix to the actual rotation matrix.

Parameters	Absolute Error		Percentage Error	
	Mean	Standard Deviation	Mean	Standard Deviation
p_{12} (m)	0.031	0.006	3.688%	0.693%
p_{23} (m)	0.027	0.008	2.867%	0.844%
p_{31} (m)	0.024	0.005	2.089%	0.458%

TABLE III: Experimental results for relative grasp frame position estimation. Each 3-vector position error is converted to a scalar using the Euclidean norm, and percentage errors are relative to the Euclidean norm of the ground truth p_{ij} .

C. Experimental Results

1) *Transformation Matrix*: The payload was moved randomly and manually in all 6-dof by a human operator using the float mode of the Omnid [1], a mode compensating for gravitational forces using active force control. The encoder data from the Omnid manipulators were collected to calculate \mathcal{V}_{i*} , $i = 1, \dots, 3$. The transformations for the individual robot pairs \hat{T}_{12} , \hat{T}_{23} , and \hat{T}_{31} were first calculated using the least-squares methods of Section III-B, and these estimates were then refined using the nonlinear optimization incorporating loop-closure constraints. (In our experiments, this second optimization step did not change the estimates significantly.) Five independent trials were conducted, each consisting of ten seconds of data (1000 samples) for the estimation process.

The errors between the estimated transformation matrices and the ground truth transformation matrices (Table I) are reported in Tables II and III for the rotation matrices and position vectors, respectively. Rotation matrix errors are expressed as the rotation angle β (in degrees) of $[\omega]\beta = \log(R_{ij}^T \hat{R}_{ij})$.

2) *Mass and Center of Mass*: To estimate the mass and center of mass of the payload, the Omnids held the payload stationary at four different orientations. The results of the least-squares estimates from Section III-C are summarized in Table IV.

3) *Inertia Matrix*: To estimate the inertia matrix, the Omnids performed four one-minute manipulation trials, with the first and last four seconds of data discarded (5200 samples for each trial). In each manipulation, two Omnid wrists moved in periodic trajectories on the surface of the sphere for which the origins of the three grasp frames lie on a common meridian. The third Omnid had its actuators locked and passively accommodated the motion of the other two Omnids via its gimbal wrist and elastic Delta joints.

Table V summarizes the results from the four experimental trials, with the estimated inertia matrix transformed into the principal axes of the payload. Similar to the labeling of axes in the ground truth inertia matrix, the labels $\hat{\mathcal{I}}_{xx}$, $\hat{\mathcal{I}}_{yy}$, and $\hat{\mathcal{I}}_{zz}$ are given to principal inertia estimates in ascending order.

Parameters	Absolute Error	Percentage Error
mass (kg)	0.099	0.867%
p_{1c} (m)	0.026	4.403%

TABLE IV: Experimental results for mass and center of mass estimation. The 3-vector position error is converted to a scalar using the Euclidean norm, and the percentage error is relative to the Euclidean norm of the ground truth p_{1c} .

Parameters	Absolute Error		Percentage Error	
	Mean	Standard Deviation	Mean	Standard Deviation
\mathcal{I}_{xx} (kg-m ²)	0.154	0.063	6.824%	2.789%
\mathcal{I}_{yy} (kg-m ²)	0.138	0.094	3.999%	2.735%
\mathcal{I}_{zz} (kg-m ²)	0.050	0.155	0.973%	2.719%

TABLE V: Experimental results of inertia matrix estimation.

V. DISCUSSION

The experimental results demonstrate the validity of the approach, producing relative grasp rotation matrix errors typically less than 3° and position vector magnitude errors of less than 4%, a mass estimate error of less than 1%, and a CoM position error of less than 5%. Inertia matrix estimation, which relies on acceleration estimates from twice-differenced encoder data, exhibits a bit more error, but it is still less than 10% for the principal moments of inertia.

The experimentally-derived kinematic and mass parameters may be directly inserted into the mocobot gravity compensation mode reported in [1], and the inertial parameters can be used to improve the performance of dynamic model-based cooperative control, eliminating the need for an *a priori* model of the payload and the grasp locations. There are a number of limitations to the method, however.

First, grasp frame velocities and accelerations are obtained by differencing encoder data, including encoders at the proximal joints of the Delta mechanism, distant from the wrist. The intervening mechanism and the differencing process introduce noise to the estimation. To address this, the Omnid sensor suite could be supplemented by IMUs at the gimbals. Independent of the sensing modality, however, the inherent compliance of the manipulators, due to their SEAs, can introduce vibrations at the wrists, which may be exacerbated by a poor choice of wrist trajectories to estimate the payload inertial properties. Because the Omnids are designed primarily for force-controlled human interaction, they are incapable of stiff, highly precise motion control, which is assumed to be supplied by the human during typical human-robot collaboration.

Second, manipulation forces at the wrist are estimated based on the Delta's proximal joint SEAs. This assumes zero friction at joints and bearings, but eliminates the need for costly and potentially fragile end-effector force-torque sensors.

Third, the limited workspace of the manipulators places constraints on the payload trajectories that can be used to determine inertial properties. In particular, the payload trajectories in our experiments were limited to less than $\pm 10^\circ$ rotation about any axis. Payload trajectories with larger rotations could provide a higher signal-to-noise ratio.

Finally, computational aspects of the method (e.g., data filtering during post-processing) could be further optimized.

VI. CONCLUSION

We present a methodology for cooperative payload estimation using a group of mobots, focusing on the estimation of the mass, center of mass, and inertia matrix of a rigid body payload, as well as the transformations between the grasp frames of each robot. The proposed method avoids the need for expensive sensors and intercommunication between robots by leveraging the twists, twist derivatives, and wrenches measured at each robot's grasp frame. Despite challenges of sensor noise and unmodeled dynamics, the proposed approach demonstrates promising results for payload estimation using Omnid mobots. Future work will focus on extending the methodology to identify the kinematic and inertial properties of articulated payloads, and eventually continuously deformable payloads.

REFERENCES

- [1] M. L. Elwin, B. Strong, R. A. Freeman, and K. M. Lynch, "Human-multirobot collaborative mobile manipulation: The omnid mobots," *IEEE Robotics and Automation Letters*, vol. 8, no. 1, pp. 376–383, 2022.
- [2] J. E. Colgate, W. Wannasuphprasit, and M. A. Peshkin, "Cobots: Robots for collaboration with human operators," in *ASME international mechanical engineering congress and exposition*, vol. 15281. American Society of Mechanical Engineers, 1996, pp. 433–439.
- [3] F. Caccavale and M. Uchiyama, "Cooperative manipulation," *Springer handbook of robotics*, pp. 989–1006, 2016.
- [4] A. Cherubini, R. Passama, A. Crosnier, A. Lasnier, and P. Fraisse, "Collaborative manufacturing with physical human-robot interaction," *Robotics and Computer-Integrated Manufacturing*, vol. 40, pp. 1–13, 2016.
- [5] J. Werfel, K. Petersen, and R. Nagpal, "Designing collective behavior in a termite-inspired robot construction team," in *Proceedings of the IEEE International Conference on Robotics and Automation (ICRA)*. IEEE, 2014, pp. 3271–3278.
- [6] J. Trevelyan, W. R. Hamel, and S.-C. Kang, "Robotics in hazardous applications," *Springer handbook of robotics*, pp. 1521–1548, 2016.
- [7] T. Balch and R. C. Arkin, "Behavior-based formation control for multirobot teams," *IEEE transactions on robotics and automation*, vol. 14, no. 6, pp. 926–939, 1998.
- [8] M. Rubenstein, A. Cornejo, and R. Nagpal, "Programmable self-assembly in a thousand-robot swarm," *Science*, vol. 345, no. 6198, pp. 795–799, 2014.
- [9] D. Rus, B. Donald, and J. Jennings, "Moving furniture with teams of autonomous robots," in *Proceedings 1995 IEEE/RSJ International Conference on Intelligent Robots and Systems. Human Robot Interaction and Cooperative Robots*, vol. 1. IEEE, 1995, pp. 235–242.
- [10] C. L. Liu, I. L. D. Ridgley, M. L. Elwin, M. Rubenstein, R. A. Freeman, and K. M. Lynch, "Self-healing distributed swarm formation control using image moments," *IEEE Robotics and Automation Letters*, 2024.
- [11] D. Sieber, S. Musić, and S. Hirche, "Multi-robot manipulation controlled by a human with haptic feedback," in *2015 IEEE/RSJ International Conference on Intelligent Robots and Systems (IROS)*. IEEE, 2015, pp. 2440–2446.
- [12] Z. Wang and M. Schwager, "Force-amplifying n-robot transport system (force-ants) for cooperative planar manipulation without communication," *The International Journal of Robotics Research*, vol. 35, no. 13, pp. 1564–1586, 2016.
- [13] C. Chi, S. Feng, Y. Du, Z. Xu, E. Cousineau, B. Burchfiel, and S. Song, "Diffusion policy: Visuomotor policy learning via action diffusion," *arXiv preprint arXiv:2303.04137*, 2023.
- [14] T. Z. Zhao, V. Kumar, S. Levine, and C. Finn, "Learning fine-grained bimanual manipulation with low-cost hardware," *arXiv preprint arXiv:2304.13705*, 2023.
- [15] Y. Ren, S. Sosnowski, and S. Hirche, "Fully distributed cooperation for networked uncertain mobile manipulators," *IEEE Transactions on Robotics*, vol. 36, no. 4, pp. 984–1003, 2020.
- [16] N. E. Carey and J. Werfel, "Collective transport of unconstrained objects via implicit coordination and adaptive compliance," in *2021 IEEE International Conference on Robotics and Automation (ICRA)*. IEEE, 2021, pp. 12 603–12 609.
- [17] A. Rauniyar, H. C. Upreti, A. Mishra, and P. Sethuramalingam, "Mewbots: Mecanum-wheeled robots for collaborative manipulation in an obstacle-clustered environment without communication," *Journal of Intelligent & Robotic Systems*, vol. 102, no. 1, p. 3, 2021.
- [18] J. Alonso-Mora, R. Knepper, R. Siegwart, and D. Rus, "Local motion planning for collaborative multi-robot manipulation of deformable objects," in *2015 IEEE international conference on robotics and automation (ICRA)*. IEEE, 2015, pp. 5495–5502.
- [19] M. P. Miller, *An accurate method of measuring the moments of inertia of airplanes*. National Advisory Committee for Aeronautics, 1930, no. 351.
- [20] A. Woodfield, "Measurement of the yawing moment and product of inertia of an aircraft by the single point suspension method theory and rig design," *Aeronautical Research Council Reports & Memoranda*, 1968.
- [21] C. B. Winkler, "Inertial properties of commercial vehicles-descriptive parameters used in analyzing the braking and handling of heavy trucks. volume 2. final report," University of Michigan Transportation Research Institute, Tech. Rep., 1983.
- [22] —, *Parametric analysis of heavy duty truck dynamic stability*. National Highway Traffic Safety Administration, 1983, vol. 1.
- [23] G. J. Heydinger, N. J. Durisek, D. A. Covert Sr, D. A. Guenther, and S. J. Novak, "The design of a vehicle inertia measurement facility," *SAE transactions*, pp. 465–473, 1995.
- [24] C. G. Atkeson, C. H. An, and J. M. Hollerbach, "Estimation of inertial parameters of manipulator loads and links," *The International Journal of Robotics Research*, vol. 5, no. 3, pp. 101–119, 1986.
- [25] G. Habibi, Z. Kingston, W. Xie, M. Jellins, and J. McLurkin, "Distributed centroid estimation and motion controllers for collective transport by multi-robot systems," in *2015 IEEE International Conference on Robotics and Automation (ICRA)*. IEEE, 2015, pp. 1282–1288.
- [26] A. Marino and F. Pierri, "A two stage approach for distributed cooperative manipulation of an unknown object without explicit communication and unknown number of robots," *Robotics and Autonomous Systems*, vol. 103, pp. 122–133, 2018.
- [27] K. M. Lynch and F. C. Park, *Modern robotics*. Cambridge University Press, 2017.
- [28] W. Kabsch, "A solution for the best rotation to relate two sets of vectors," *Acta Crystallographica Section A: Crystal Physics, Diffraction, Theoretical and General Crystallography*, vol. 32, no. 5, pp. 922–923, 1976.
- [29] —, "A discussion of the solution for the best rotation to relate two sets of vectors," *Acta Crystallographica Section A: Crystal Physics, Diffraction, Theoretical and General Crystallography*, vol. 34, no. 5, pp. 827–828, 1978.
- [30] S. Umeyama, "Least-squares estimation of transformation parameters between two point patterns," *IEEE Transactions on Pattern Analysis & Machine Intelligence*, vol. 13, no. 04, pp. 376–380, 1991.
- [31] J. Nocedal and S. J. Wright, "Large-scale unconstrained optimization," *Numerical optimization*, pp. 164–192, 2006.
- [32] S. Thrun, W. Burgard, and D. Fox, *Probabilistic Robotics*. Cambridge, MA: MIT Press, 2005.
- [33] F. Lu and E. Milios, "Globally consistent range scan alignment for environment mapping," *Autonomous robots*, vol. 4, pp. 333–349, 1997.